

pubs.acs.org/journal/abseba Article

Delivery of Immobilized IFN- γ With PCN-333 and Its Effect on Human Mesenchymal Stem Cells

Josh Phipps, Mahsa Haseli, Luis Pinzon-Herrera, Ben Wilson, Joshua Corbitt, Shannon Servoss, and Jorge Almodovar*



Cite This: https://doi.org/10.1021/acsbiomaterials.2c01038



ACCESS

Metrics & More

Article Recommendations

IMMUNOMODULATION POTENTIAL

High

Low

Activated anti-inflammatory hMSC

V IFN

MOF + IFN

MOF + IFN

ABSTRACT: Interferon-gamma (IFN- γ) plays a vital role in modulating the immunosuppressive properties of human mesenchymal stem/stromal cells (hMSCs) used in cell therapies. However, IFN- γ suffers from low bioavailability and degrades in media, creating a challenge when using IFN- γ during the manufacturing of hMSCs. Metal—organic frameworks (MOFs), with their porous interiors, biocompatibility, high loading capacity, and ability to be functionalized for targeting, have become an increasingly suitable platform for protein delivery. In this work, we synthesize the MOF PCN-333(Fe) and show that it can be utilized to immobilize and deliver IFN- γ to the local extracellular environment of hMSCs. In doing so, the cells proliferate and differentiate appropriately with no observed side effects. We demonstrate that PCN-333(Fe) MOFs containing IFN- γ are not cytotoxic to hMSCs, can promote the expression of proteins that play a role in immune response, and are capable of inducing indoleamine 2,3-dioxygenase (IDO) production similar to that of soluble IFN- γ at lower concentrations. Overall, using MOFs to deliver IFN- γ may be leveraged in the future in the manufacturing of therapeutically relevant hMSCs.

KEYWORDS: metal-organic framework, drug delivery, hMSCs, interferon-gamma

■ INTRODUCTION

Recent years have seen a significant increase in the study of metal-organic frameworks (MOFs) since their foundational introduction by Omar Yagi and co-workers.¹⁻⁷ These porous crystalline particles are often produced on the nanoscale and due to their interchangeable parts, are vastly customizable. This ability to selectively choose components and synthesize tailor-made MOFs allows these particles to be functionalized as well as have their three-dimensional size and shape manipulated.^{3,8} This is further promoted by the open pores and large surface areas of MOFs which allow materials to move into the particles providing a high loading capacity and surface area.8 This effect is excellent for reactions, allowing the free flow of reactants and products to reaction sites. This trait has also been exploited to encapsulate or trap objects, which can be as big as proteins or as small as gas particles, making MOFs prominent devices for gas storage, drug delivery, and protein immobilization and/or encapsulation.

Protein immobilization and encapsulation is made possible by the fluid nature of proteins with their ability to fold and unfold as well as the inherent interactions arising between the chemical groups on MOF particles and the proteins. Immobilization is a relatively simple process where the charged portions of proteins interact with the positively charged bare node sites on the framework and become coordinated to that site. ^{9,10} Encapsulation is a more complicated process where the protein either moves into the framework via diffusion or is placed in solution with MOF reactants and the framework is built up around it. The former is called postsynthetic

Received: September 1, 2022 Accepted: December 19, 2022



encapsulation (PSE) and the latter is known as Denovo encapsulation or DNE. ¹¹ In both PSE and DNE, proteins are held in place physically by the surrounding framework, but they are also held in place by intermolecular forces such as London dispersion forces (LDFs), dipole—dipole interactions, and hydrogen bonding between the framework and the protein. ¹⁰,12

Protein immobilization and encapsulation using MOFs has been shown to allow improved reaction kinetics while protecting the housed protein from extreme conditions that would otherwise cause the protein to denature and become inactive. This includes reactions taking place at temperatures above 60 °C, in organic solvents, and at both high and low pH. We demonstrate this effect in a recent publication encapsulating and monitoring the loading and reaction kinetics of alcohol dehydrogenase in the MOF PCN-333(Fe). While catalytic reactions are a major interest in MOF-protein immobilization using biocompatible MOFs, another key use of is in drug and protein delivery. An excellent example is provided in a recent work by Luzuriaga et al., where it is shown that proteinaceous vaccines can be both protected/insulated from the outside environment as well as carried by site-directed delivery to a given location even inside the cell.

The delivery of proteins is a very promising area of study with the ability to have a dramatic impact. Human mesenchymal stem/stromal cells (hMSCs) are an excellent model cell and are particularly interesting to cellular therapy programs due to their function as an immunosuppressant. During tissue damage, hMSCs have the ability to secrete paracrine and anti-inflammatory factors to repair tissue. In addition, hMSCs contribute not only to the repair of damaged tissues but also possess remarkable immunomodulatory activity by producing anti-inflammatory and immunosuppressive factors. This has led to hMSCs becoming a promising tool for new medical applications and therapies in the treatment of diverse diseases and disorders, such as graft-versus-host disease (GVHD), inflammatory diseases, and autoimmune disorders.

It has been shown that the immunosuppressive properties of hMSCs rely on the existence of IFN- γ in the microenvironment.²⁷ This signaling protein is a potent pro-inflammatory cytokine produced by CD4+ lymphocytes, natural killer cells (NKT) cells, and macrophages. Because of this function, IFN-γ plays an essential and complex role in innate and adaptive immune responses toward viral infections, bacteria, protozoa, and GVHD. 28,29 A recent study by Croitoru-Lamoury et al. showed that IFN-y has the ability to modulate the immune properties and differentiation potential of hMSCs.³¹ While this presence of IFN- γ increases the immunosuppressive properties of hMSCs, the transient effects of IFN- γ may limit the potential of hMSCs to modulate immune responses for more than a few days in cell environments that do not expose the cells to adequate concentrations of IFN-y, such as in chronic inflammatory states.³⁵ Therefore, providing a means of locally concentrating and sustaining the presentation of IFN-y to hMSCs may significantly enhance the immunomodulatory potential of the cells. A recent study by Zimmerman et al. illustrated this effect and showed that heparin based nanoparticles could be used to deliver IFN-y and demonstrated increased IDO expression and improved immune suppressive properties.³⁵ MOFs having proven themselves as an effective and biocompatible tool for drug delivery may aid this process through its own unique characteristics. In this paper we seek to

show that the immobilization, protection from degradation, and delivery of factors, specifically IFN- γ with PCN-333(Fe) to the local extracellular environment is an effective means for delivery to potentiate hMSC immunomodulatory activity.

■ EXPERIMENTAL SECTION

Synthesis of PCN-333(Fe). The precursor 4,4′,4″-s-triazine-2,4,6-triyl-tribenzoic acid (H_3 TATB) and MOF PCN-333(Fe) were synthesized according to the method described in the work by Park et al. 2015. The in a 15 mL reaction vessel, we combined 60 mg of H_3 TATB, 60 mg of anhydrous FeCl $_3$ (III), 0.6 mL of TFA, and 10 mL of dimethylformamide. The vessel was then sealed and placed in an oven at 150 °C for 12 h. A brown precipitate formed and was collected by centrifugation. The product was washed several times each by dimethylformamide, acetone, and water with centrifugation after each step to collect. Water was then exchanged with acetone three times before activation in an oven at 70 °C overnight. The product was then confirmed via X-ray diffraction using a Rigaku MiniFlex II. The size and shape were also determined via the use of a Horiba LA-950 particle size analyzer and scanning electron microscope (SEM), respectively.

Immobilization of IFN- γ with PCN-333(Fe). A loading solution of PCN-333 and IFN- γ was combined with a final concentration 0.1 mg/mL IFN- γ and either 0.5 or 1 mg/mL PCN-333 depending on the test. This solution was vortexed and allowed to sit at 4 °C for 24 h. The solution was then removed after gentle centrifugation leaving the immobilized IFN- γ and PCN-333. Percent immobilization was determined using ultra violet—visible (UV—vis) absorption of an aliquot of the supernatant at 395 nm.

Experimental Design. In this work, the effects of MOF concentration and presence or absence of recombinant human IFNγ (ThermoFisher, Cat. #PHC4031) immobilized with the MOF in culture medium were studied and their effect on the hMSCs are reported. Six test conditions were examined including a negative control group lacking IFN-γ (-IFN-γ), a positive control group $(+IFN-\gamma)(50 \text{ ng/mL})$, and test groups containing either 0.5 or 1 mg/ mL MOF with and without IFN-γ immobilized. The choice in concentration of our control was selected based on our previous works. 32,37 Cell media containing MOF was created by placing MOF (either loaded with IFN-y or bare) in 15 mL of media in a 15 mL centrifuge tube and subsequently vortexed before addition to cells soon after and had a final concentration of 14.2 ng/mL for the 0.5 mg/mL MOF sample and 14.4 ng/mL for the 1 mg/mL sample. Conditions will hereafter be referred to as "control groups" containing media with and without IFN- γ (\pm) and "test groups" containing MOF at a concentration of either 0.5 or 1 mg/mL with or without IFN-y loaded.

hMSC Viability. For hMSC viability, the PrestoBlue cell viability assay from Invitrogen (Cat. #A13261) was used. hMSCs (10 000 cells/cm²) were seeded on a 96 well-plate, and cell viability was measured after 3 and 6 days of culture with control groups and test groups containing. This viability testing was conducted as we have described in our previous works. ^{37–40} Following propagation, the cell culture medium was removed, and 100 μ L of solution was added per well containing 90% fresh cell medium and 10% PrestoBlue reagent. The plate was then incubated for 3 h, and the fluorescence intensity was measured using a BioTek multi-mode microplate reader (model Synergy 2) with excitation/emission of 560/590 nm. Data were reported as the average with standard deviation shown from experiments with 4 wells per condition.

Cell nuclei and actin cytoskeleton were stained using the fluorescent dyes Hoechst 33342 which was purchased from Invitrogen (ref. #H3570) and ActinRed 555 Ready Probest (Invitrogen, ref. #37112). After 3 days of culture, the cell medium was removed, and the cells were fixed with 4% formaldehyde solution for 15 min. The samples were washed several times with PBS followed by the addition of Triton X100 for 10 min before being washed 3 times with PBS. ActinRed 555 was first added and incubated for 30 min. Then, Hoechst 33342 was added for 10 min and protected from light using

aluminum foil. Both dyes were washed 5 times with PBS before and after being added. For cell imaging, a Leica inverted fluorescence microscope was used with a standard DAPI filter (excitation/emission of 350/461 nm) for Hoechst 33342, and a standard TRITC filter (excitation/emission of 540/565 nm) for ActinRed 555.

Real-Time Monitoring of hMSC Behavior. An xCELLigence Real-Time Cell Analyzer (RTCA S16) instrument from ACEA Biosciences Inc. (Cat. #00380601430) was used to measure real-time cell behavior. hMSCs at a concentration of 5000 cells/cm² were seeded on the wells of an ACEATM E-Plate L16 (Cat. #00300600890, cell growth area of 0.32 cm² per well), on both control groups and test groups. The xCELLigence instrument was configured as described in our previous works. ^{37,38} Briefly, the xCELLigence RTCA S16 was placed inside the incubator to allow the device to warm up for at least 2 h before use. The RTCA S16 was set up to perform readings every 10 min for a period of 72 h of cell culture.

Immunomodulatory Factor Expression of hMSCs. For the hMSC immunomodulatory factor expression, hMSCs (5000 cells/ cm²) were seeded on each well of a 24 well-plate using the previously mentioned control and test conditions, and the IDO activity was measured after 3 and 6 days of culture as described in our previous works. 37,39,41 Briefly, 100 μ L of cell supernatant was mixed with 100 μ L of standard assay mixture consisting of (potassium phosphate buffer (50 mM, pH 6.5), ascorbic acid (40 mM, neutralized with NaOH), catalase (200 μ g/mL), methylene blue (20 μ M), and Ltryptophan (400 μ M)). The mixture was kept at 37 °C in a humidified incubator with 5% CO₂ for 30 min (in a dark environment to protect solutions from light) to allow IDO to convert L-tryptophan to N-formyl-kynurenine. After that, the reaction was stopped by adding 100 µL of trichloroacetic acid 30% (wt./vol.) and incubating for 30 min at 58 °C. After hydrolysis of N-formyl-kynurenine to kynurenine, 100 μ L of mixed cell supernatant/standard transfer into a well of a 96-well microplate, followed by adding 100 μ L per well of 2% (w/v) p-dimethylaminobenzaldehyde in acetic acid. The absorbance was read at 490 nm at the end point using a BioTek Synergy 2 spectrophotometer (Synergy LX multi-mode reader from BioTek model SLXFA).

hMSC Differentiation. hMSC differentiation was induced by exchange of culture with differentiation media (Osteogenic and Adipogenic media). Control cultures were grown in a regular cell expansion medium. Briefly, hMSCs (10 000 cells/cm²) were seeded with each testing condition prepared on 24-well plates and grown for 6 days in expansion medium (MEM Alpha (1x) supplemented with L-glutamine, ribonucleosides, and deoxyribonucleosides) containing 20% fetal bovine serum, 1.2% penicillin-streptomycin, and 1.2% Lglutamine at 37 °C in a humidified incubator with 5% CO₂. After the cells reached at least 50% confluency, they were exposed to a differentiation medium. For osteogenic differentiation, hMSCs were cultured in the differentiation medium (DMEM low glucose, 10% fetal bovine serum,1% penicillin, 1% L-glutamine, 50 μM ascorbic acid (50 mg/10 mL)) (Sigma, Cas Number: 50-81-7), 10 mM β glycerophosphate (Sigma, CAS Number: 154804-51-0, G9422), and 100 nM dexamethasone (Sigma, CAS Number 50-02-2). The medium was replaced every 2-3 days. After 8 days of culture, cells were fixed with 10% formaldehyde. For osteogenic differentiation, Alizarin Red S (Sigma, CAS Number 130-22-3) staining solution was prepared by adding 2 g of Alizarin Red S in 100 mL of wate rand mixing. The pH was adjusted to 4.1-4.3 by the addition of ammonium hydroxide, as necessary. Alizarin Red S solution was added to the fixed cells, then incubated at room temperature in the dark (cover with aluminum foil) for 15 min. The staining solution was removed and rinsed 3 times with PBS. The samples were analyzed immediately under the microscope to detect calcium deposits. For adipogenic differentiation, hMSCs were cultured in the differentiation medium consisting of DMEM high glucose supplemented with 10% fetal bovine serum, 1% penicillin, 1% L-glutamine, 1 μ M dexamethasone (Sigma, CAS Number 50-02-2), 0.01 mg/mL insulin (Sigma-Aldrich, Catalog No. I2643), 0.5 mM 3-isobutyl-1-methylxanthine (IBMX) (Sigma, CAS Number: 28822-58-4, I5879), and $100 \mu M$

indomethacin (Sigma, CAS Number: 53-86-1). The medium was replaced every 2-3 days. After 8 days of culture, cells were fixed with 10% formaldehyde, stained with 0.5% (w/v) Oil Red O (Sigma-Aldrich, Catalog Number: O0625) in 100% isopropanol, and incubated at room temperature for 30 min and protected from light. The cell monolayer was washed 2 times with PBS. The sample was analyzed under a light microscope to detect lipid vesicles that appeared in bright red.

Effect of IFN-γ and PCN-333 on hMSC Protein Expression. Protein expression was determined using a Luminex MAGPIX and the Invitrogen Th1/Th2 Cytokine 11-Plex Human Kit (Assay ID: EPX110108010). The cells tested were seeded at a density of 5000 cells/cm² in a 24-well plate. After 3 days of culture, 500 μ L of supernatant from the culture medium of each test and control group was collected. The samples were stored in a freezer at -80 °C. On the day of reading, the samples were slowly thawed on ice, vortexed for 30 s, and then centrifuged at 2000 g for 1 min. Following this, 50 μ L of each sample was analyzed according to the kit protocol. A total of 11 analytes were determined in this study.

Error of the Mean. A one-way analysis of variance (ANOVA) performed comparisons among multiple groups. A *p*-value <0.05 was considered statistically significant. The statistical analysis was done using SigmaPlot software version 14.

RESULTS AND DISCUSSION

Characterization of PCN-333(Fe). The successful synthesis of PCN-333(Fe) was confirmed via powder X-ray diffraction, showing a pattern consistent with previous works (Figure 1a). The product was then observed under SEM (Figure 1b), which shows that the product is roughly spherical in nature. Upon size analysis using the Horiba LA-950, it was determined that the average particle size was $17.8~\mu m$ while the mode was $18.6~\mu m$. The standard deviation was determined to be 2.7.

Immobilization of IFN- γ with PCN-333(Fe). To immobilize IFN- γ , a solution of 0.1 mg/mL IFN- γ and either 0.5 or 1 mg/mL PCN-333 in 20 mM pH 7 HEPES buffer was prepared. The solution was lightly vortexed and allowed to sit at 4 °C for 24 h. The solution was then lightly vortexed and subsequently centrifuged at 1000 g for 1 min. The supernatant was removed, and the sample was ready for incorporation into the cell media. Percent immobilization was then determined by absorbance of the supernatant at 280 nm against controls via Bradford Assay using UV—vis spectrometry. This showed the percent immobilization to be 63.9% for the 0.5 mg/mL loading and 65.0% for the 1.0 mg/mL sample.

PrestoBlue Viability Assay. Cytotoxicity was evaluated by monitoring the activity of the reagent Presto Blue after all conditions reached full confluency (Figure 2a). Using this reagent, cell viability was measured after 3 and 6 days of culturing hMSCs cells under each condition as described in the experimental design. Those conditions being with and without IFN- γ supplemented in the culture medium, MOF (0.5 mg/ mL), MOF (0.5 mg/mL) + IFN- γ , MOF (1 mg/mL), and MOF (1 mg/mL) + IFN- γ . The negative control group selected contained cell medium lacking IFN-y. The fluorescence intensity of this control was normalized to 100%, and all other conditions were assessed in relation to this control group at 3 days and 6 days, respectively. Figure 2b shows that the presence of IFN- γ in the cell medium yields an increased cell viability of 5% and 11% compared to the control at 3 and 6 days, respectively. This 3 day result was not statistically different from the control (P > 0.05) and shows that IFN- γ itself does not significantly affect cell viability in the short term; however, over a longer period, it appears to have a promoting

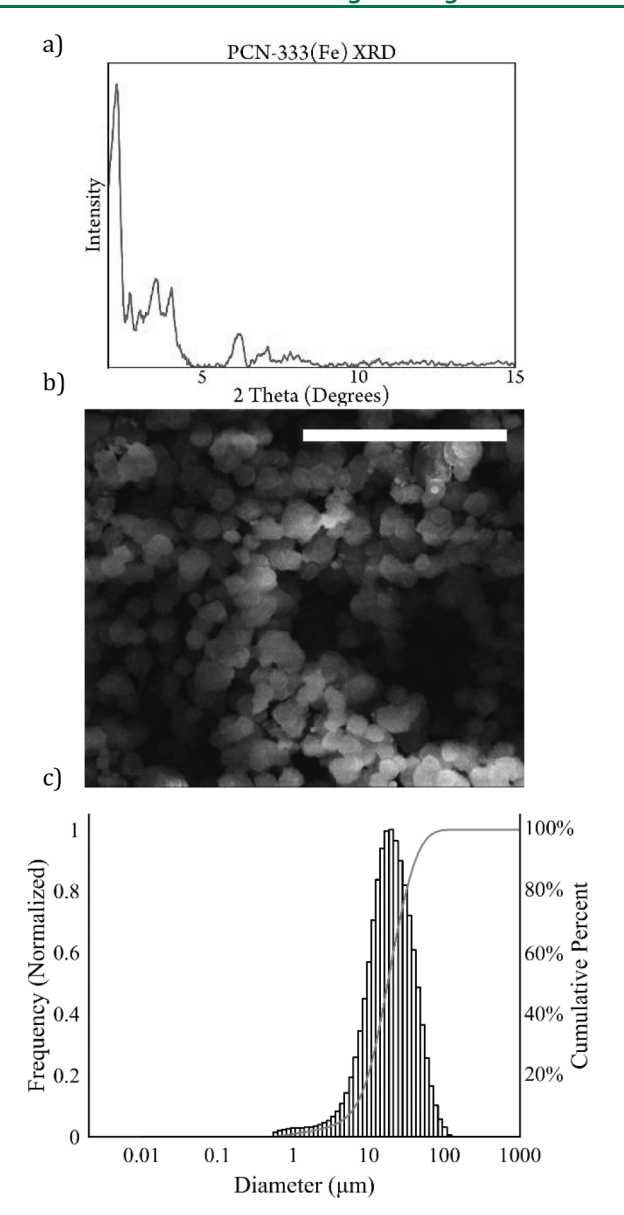


Figure 1. (a) pXRD of synthesized PCN-333 (Fe), (b) SEM image of synthesized PCN-333(Fe) with scale bar representing 40 μ m, (c) size distribution of synthesized PCN-333(Fe) (black) and cumulative percentage of product (red).

effect. In contrast to this, the addition of MOF at both concentrations after 3 days showed a statistically significant increase in cell viability, with the 0.5 mg/mL sample yielding a 14.5% increase and the 1 mg/mL sample yielding a 6.7% increase (P < 0.05). This suggests that MOF alone when present in media may improve cell viability. The reason for this is presently not clear. Apart from these results, all other data points did not statistically deviate from the control group and although there appears to be a decrease in the 1 mg/mL MOF sample at 6 days, this can be attributed to a slower growth rate, as the value is in relation to the control group, which slightly surpassed it in cell number. In regard to the MOF samples, these data indicate that they do not present a cytotoxic threat to hMSCs, making them suitable carriers.

Real-Time Monitoring of Cell Behavior and Proliferation. In this study, hMSCs at 25,000 cells/cm² were cultured on E-Plate 16 to evaluate the real-time behavior of the cells during the first 72 h of culture. The effect of control and test

group media on these cells was evaluated. An xCELLigence RTCA S16 biosensor system was used to measure cell proliferation and growth. This system constantly measures the impedance difference caused by cells attached to microsensors present in culture plates (E-plates 16) and is monitored by microchips attached under the wells. In this way, the impedance difference is translated into a parameter known as the cell index (CI). Therefore, the higher the CI, the greater the number of cells are adhered and present on the bottom of the well.³⁸ Based on our previous study, our results indicate two cell behavior phases: a cell adhesion (hours 0–20) and a cell growth phase (hours 20–50).⁴¹ In this test, we used a similar cell density to our previous work, which is also recommended by the manufacturer.³⁸

Figure 3 shows the CI values as a function of the first 50 h of culture for the test and control groups. The figure shows a cell adhesion stage in the evaluated period, reaching a maximum peak at approximately 9 h. CI values reached a maximum of 8 CI units. Compared to the samples with IFN- γ present, those lacking IFN-γ showed a slightly lower CI value, which may correspond to slightly fewer cells adhering and is consistent with a recent study that showed that IFN-γ can lead to improved cell adhesion. 43 The decrease in CI between hours 9 and 20 corresponds to possible cell detachment and rearranging. Beyond hour 20, the CI index begins to increase slightly, corresponding to a slow growth phase. These results indicate that the hMSCs have a similar adhesion and growth behavior in all of the conditions evaluated. This is in agreement with our PrestoBlue data, that MOF at both concentrations and with or without IFN-y does not negatively affect cell adhesion. Regarding cell growth, there was little growth measured between hours 20 and 50. This performance could be because of the rapid increase in cell adherence observed in the first 10 h, leading to a confluence close to 100% in a short

IDO Assay. Indoleamine 2,3-dioxygenase (IDO) is a cytosolic heme protein important for immuno-regulatory functions. 42,44 Its presence can be evaluated by measuring the concentration of kynurenine, which is a known catalyzer that helps convert L-tryptophan to kynurenine. 44,45 The ability of IFN- γ to induce IDO expression in hMSCs was compared using the control and test groups and results were gathered after 3 days and 6 days. These results for IDO activity are summarized in Figure 4, which shows that IFN- γ supplemented in cell medium increases the IDO activity by roughly 3 times when compared to the cell medium without IFN- γ . These results are in line with the study done by Kwee et al., indicating the IDO activity was correlated with the amount of IFN- γ present. 46

With regard to the bare MOF (0.5 and 1 mg/mL) in cells medium, the results show no statistical differences when compared to the negative IFN- γ control. This indicates that MOF alone does not induce IDO activity. Also, both of the loaded MOF samples showed an increase in IDO activity that was consistent to that of the positive IFN- γ control (P < 0.05). This supports our claim that IFN- γ was successfully incorporated with the MOF particles in agreement with our Bradford Assay results. It also shows that, although a smaller portion of IFN was loaded into the framework and provided to the cells in media compared to the control (50 ng/mL in the control vs ~14 ng/mL loaded into MOF), there was an equivalent production of IDO. This result suggests that the immobilization of IFN- γ and its localized delivery to hMSCs

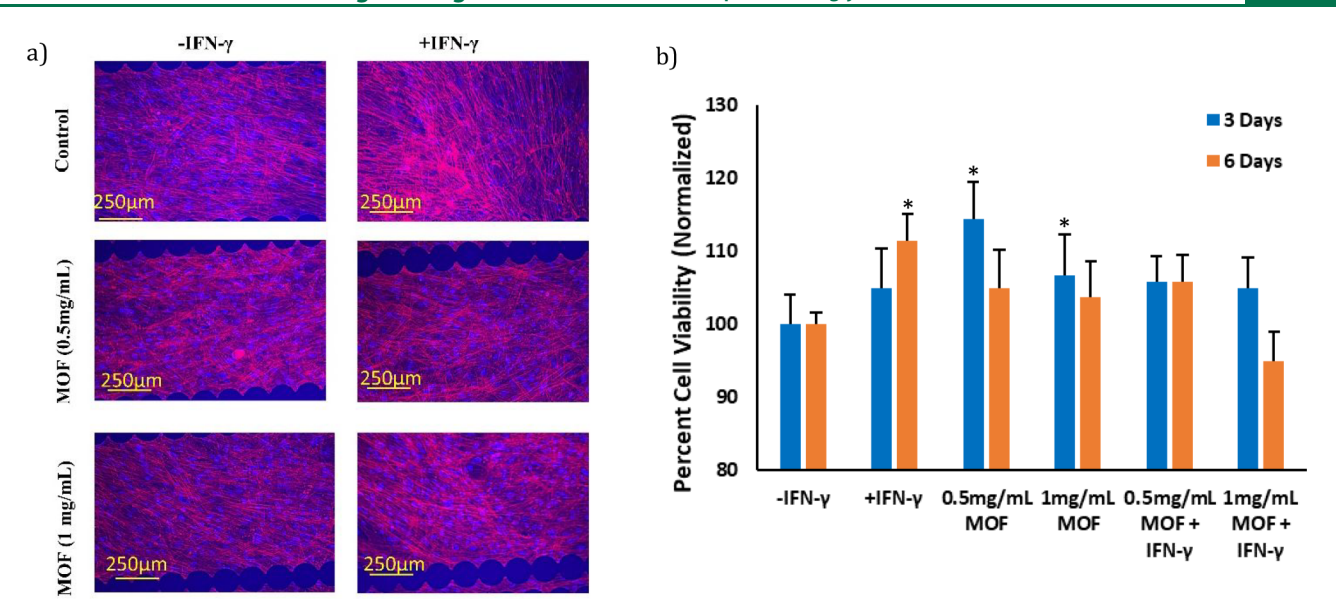


Figure 2. (a) Fluorescence microscopy images of hMSCs nuclei and actin cytoskeleton, labeled with Hoechst and Actin Red. (B) PrestoBlue Viability assay for cultured hMSCs after 3 and 6 days with each group normalized against their respective control (-IFN- γ) and with significant differences (P < 0.05) compared to that of the control denoted with an asterisk.

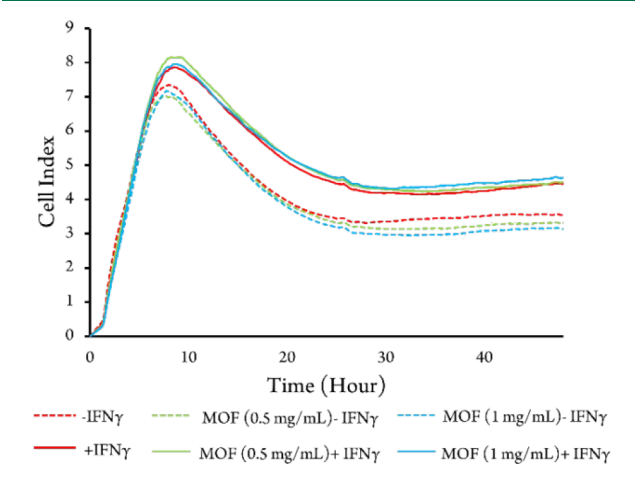


Figure 3. Real-time monitoring of hMSCs after 72 h using xCELLigence.

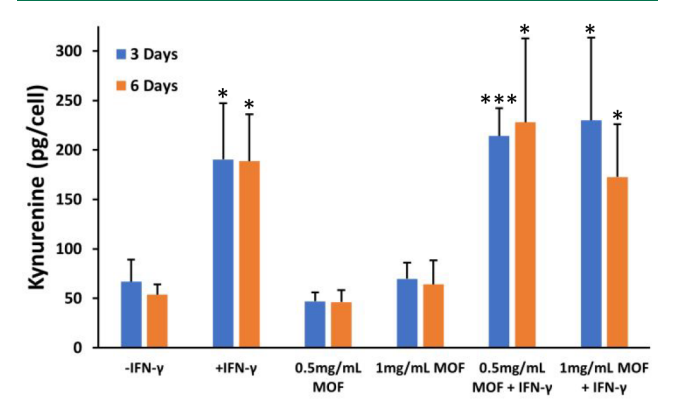


Figure 4. Cell immunomodulatory potential by IDO activity for hMSCs as a measure of picograms of kynurenine produced by cells cultured after 3 and 6 days with significant differences from respective controls marked accordingly (*P < 0.05 and ***P < 0.005).

provides a more bioavailable and active source than that of free IFN- γ in solution. In addition, the MOF (0.5 mg/mL) + IFN- γ

sample shows consistent IDO activity between both the 3 day and 6 day results. The same is true for the test using MOF (1 mg/mL) + IFN- γ at 3 days. These results indicate that the MOF at these concentrations and time period do not inhibit the release of IFN-γ. There was, however, a minor contrast in the test using MOF (1 mg/mL) + IFN- γ at 6 days. Although there was no statistical difference, a decrease in the average amount of IDO was present when compared to the positive control. This difference may be related to the amount of IFN-γ encapsulated in MOF when compared to the actual MOF concentration and can be expected when there are more potential binders in solution, given that there are twice the amount of MOF particles. Meaning that some IFN- γ released by the particles could have been immobilized again on another particle, thus, leading to this decreased affect. Together, these results indicate that MOFs have the ability to release IFN-y through passage of time and can provide excellent bioavailability of loaded IFN- γ to the localized cellular environment, significantly surpassing the efficiency of free IFN- γ in solution.

Cell Differentiation Assay. The ability of hMSCs to differentiate into osteogenic and adipogenic lineages cells was induced by replacing the growth medium with the differentiation medium. The differentiation ability of hMSCs was evaluated to confirm the multipotentiality of hMSCs. After 10 days of incubation, cell functions associated with osteoblast differentiation (calcium deposition) and adipogenic differentiation were evaluated. Mineralization was also characterized from microscope images.

Figure 5 shows that there are areas visible with red and purple, indicating the formation of the calcified regions and adipocyte-like cells, respectively. Figure 5 also shows that control cells show a calcium deposit formed by the clustering of cells due to the strong staining with Alizarin red even with and without IFN- γ , which indicates osteogenic differentiation of cells. The same results were found for MOF (0.5 and 1 mg/mL) and MOF (0.5 and 1 mg/mL) + IFN- γ , as shown in Figure 5. This figure also shows that control cells, even with and without IFN- γ have the ability to differentiate into adipogenic cells, which the cells changed from long spindle-

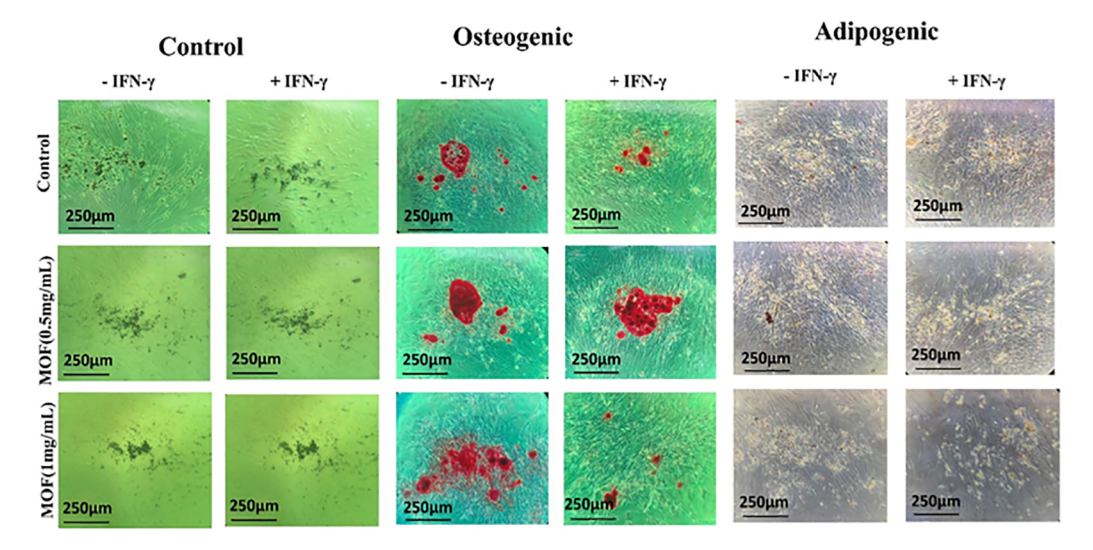


Figure 5. hMSC differentiation. Control cells inducing by normal expansion medium (left). Osteogenic differentiations were stained by Alizarin Red (center). Adipogenic differentiations were stained by Oil Red (right).

shaped to flattened round or polygonal cells. In addition, the treatment with IFN- γ encapsulated in MOFs shows no inhibitory effect on the osteogenic and adipogenic differentiation of hMSCs, and no staining was observed on cells cultured in regular expansion medium.

Effect of IFN-\gamma and PCN-333 on hMSC Protein Expression. To determine the effect of the introduction of IFN- γ and MOF particles on the expected protein expression of hMSCs, we conducted a protein expression test. In doing so, a total of 11 cytokines were monitored for this assay. The five test conditions including the presence and/or absence of IFN- γ and MOF were analyzed, and the resulting concentration of the cytokines was obtained in pg/mL. A Z-score for each analyte can be observed in a heat map provided in Figure 6 and an accompanying table of values has been provided in Table S1.

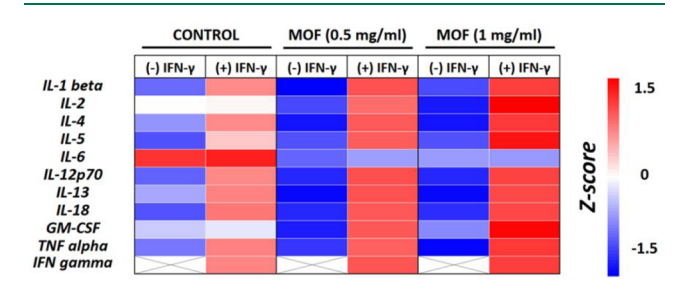


Figure 6. hMSC protein expression potential as a response of 3 days of cell culture under various conditions. Heatmap shows the Z-score values of 11 human cytokines. Data are presented as the mean of n = 5 samples.

After 3 days of cell culture, the control group containing IFN- γ showed a considerable increase in the concentration of all the analytes except for IL-6 compared to the negative control. These results demonstrate, in agreement with recent work by Garcia et al., that the presence of IFN- γ produces a favorable effect on hMSC protein expression. This increase in Z-value by the control group was surpassed by the test groups containing IFN- γ immobilized with PCN-333 and showed a direct correlation between the concentration of MOF and the resulting Z-value, indicating that the presence of

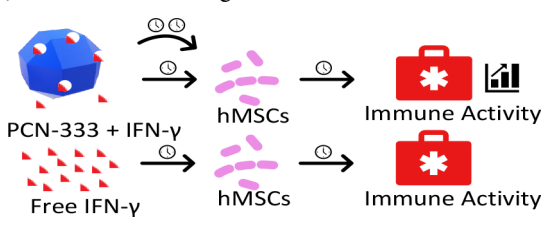
MOF in this process was contributing to amplified expression. Specifically, the IFN- γ immobilized on MOF resulted in increased expression of IL-2, GM-CSF, and TNF alpha in a ratio of about 1.5 times higher than that of the positive control, increases in IL-1 beta, IL-4, IL-12p70, and IL-13 were slightly more than doubled, and expression of IL-5 and IL-18 was over five times greater. In contrast to this, IL-6 expression decreased with the addition of MOF and was not affected as IFN- γ was introduced, indicating that its expression was independent from IFN- γ .

Although IL-6 acts dually as a pro- or anti-inflammatory cytokine, hMSCs have been shown to activate its immuno-suppressive role. Therefore, a decrease in the expression of IL-6 can be attributed as a favorable result for the immune response of hMSCs. This decrease in expression as MOF was introduced was not unique to IL-6 as the presence of bare MOF resulted in a decrease across the board to all proteins. This can be attributed to the extensive sink created with the addition of MOF as its presence introduces a severe depression in the distribution of extracellular components owing to its large inner pores. This will result in the soaking up of nearby molecules to satisfy diffusion principles in solution and is commonly known as the "sponge effect" and is the mechanism responsible for the loading of particles into the framework.

Finally, IFN-γ concentration was also determined for all culture conditions. Samples containing IFN-γ showed approximately 1900, 23 400, and 25 400 pg/mL for positive control, MOF 0.5 mg/mL, and MOF 1 mg/mL, respectively, after this 3 day period. For this condition, an initial concentration of 50,000 pg/mL was dissolved in the cell media for the control group; therefore, our results indicate that the amount of IFN-7 decreases over time due to transient effects in the presence of hMSCs.35 These can include protein degradation or consumption by cells. Alternatively, this sharp decrease in concentration is not observed in the presence of MOF particle. These results agree with recent studies showing that IFN-y immobilization can lead to an increased immunological response.35,48 They also indicate that MOFs can be applied to locally concentrate and provide sustained release of bioactive IFN-γ to potentiate hMSC immunomodulatory activity. 35 Additionally, the proteins selected for this panel were specifically chosen due to their role in the immune

response, providing evidence that this proposed synergistic effect using MOF to promote downstream proteins could be utilized as an instigator in applications to promote more efficient wound healing. A schematic overview of this process has been provided in Scheme 1, where the increased

Scheme 1. Experimental Overview Depicting the Proposed Sustained Release and Improved Immunological Activity of IFN- γ Immobilized Using PCN-333



concentration of IFN- γ in solution compared to that loaded into the MOF, the release over time from the MOF (where the clock represents a time unit), and the improved immune activity promoted as a result of the immobilization of IFN- γ on PCN-333 are shown.

CONCLUSIONS

In this work, we tested the viability of the metal-organic framework PCN-333(Fe) as a carrier device for the local extracellular delivery of IFN-y to hMSCs and monitored their immunomodulatory activity to determine efficacy. From our results, we show that, likewise to other publications, the PCN-333(Fe) has little to no effect on cell viability and the particle does not present signs of cytotoxicity. Additionally, when introduced to the cell differentiation assay, the experimental group containing the MOF particles showed no variance and continued to differentiate appropriately. When measuring the efficiency of IFN-γ to induce IDO, in the presence of MOF, the controls containing only the particle had no effect showing it to be an ideal carrier, not interfering with the biological pathways and, in fact, showed a slight promoting effect on cell viability at 3 days. When the immobilized IFN- γ with MOF was examined, although it had a lower IFN- γ content relative to the control group (~14 ng/mL vs 50 ng/mL, respectively), it did not have a significant decrease in IDO activity and yielded an increase in the expression of proteins related to immune response exceeding that of the free IFN-γ control. This successful action of immobilized IFN-γ compared to the control group over the course of 3 and 6 days shows that PCN-333(Fe)(and likely other MOFs) is a suitable delivery device for small proteins and drugs to the localized cellular environment with no significant side effects on the surrounding environment or the cellular ability to reproduce/differentiate and has the added benefit of providing a sustained release of loaded materials to nearby cells. Future studies will be needed to further understand the viability of this delivery method, but the results from this work suggest that the use of MOFs as a delivery device is a reasonable alternative to conventional methods of drug delivery.

ASSOCIATED CONTENT

Supporting Information

The Supporting Information is available free of charge at https://pubs.acs.org/doi/10.1021/acsbiomaterials.2c01038.

Raw data for multiplex assay (PDF)

AUTHOR INFORMATION

Corresponding Author

Jorge Almodovar — Cell and Molecular Biology Graduate Program and Ralph E. Martin Department of Chemical Engineering, University of Arkansas, Fayetteville, Arkansas 72701, United States; ● orcid.org/0000-0002-1151-3878; Email: jlalmodo@uark.edu

Authors

Josh Phipps — Cell and Molecular Biology Graduate Program, University of Arkansas, Fayetteville, Arkansas 72701, United States

Mahsa Haseli — Ralph E. Martin Department of Chemical Engineering, University of Arkansas, Fayetteville, Arkansas 72701, United States; oorcid.org/0000-0002-6593-6139

Luis Pinzon-Herrera — Ralph E. Martin Department of Chemical Engineering, University of Arkansas, Fayetteville, Arkansas 72701, United States

Ben Wilson – Ralph E. Martin Department of Chemical Engineering, University of Arkansas, Fayetteville, Arkansas 72701, United States

Joshua Corbitt – Ralph E. Martin Department of Chemical Engineering, University of Arkansas, Fayetteville, Arkansas 72701, United States

Shannon Servoss – Ralph E. Martin Department of Chemical Engineering, University of Arkansas, Fayetteville, Arkansas 72701, United States

Complete contact information is available at: https://pubs.acs.org/10.1021/acsbiomaterials.2c01038

Author Contributions

The manuscript was written through contributions of all authors. All authors have given approval to the final version of the manuscript.

Notes

The authors declare no competing financial interest.

ACKNOWLEDGMENTS

This work was financially supported in part by the National Science Foundation under grant no. 2051582 and by the University of Arkansas Cell and Molecular Biology Graduate Program by providing J.P. with a scholarship. The authors thank the Arkansas Nano & Biomaterials Characterization Facility for their assistance with SEM. The authors thank the University of Arkansas Chemistry Department for access to the XRD.

ABBREVIATIONS

DNE, denovo encapsulation; PSE, postsynthetic encapsulation; IFN- γ , interferon gamma; hMSC, human mesenchymal stem cell

REFERENCES

- (1) Eddaoudi, M.; Li, H.; Yaghi, O. M. Highly Porous and Stable Metal—Organic Frameworks: Structure Design and Sorption Properties. *J. Am. Chem. Soc.* **2000**, 122 (7), 1391–1397.
- (2) Kim, J.; Chen, B.; Reineke, T. M.; Li, H.; Eddaoudi, M.; Moler, D. B.; O'Keeffe, M.; Yaghi, O. M. Assembly of Metal—Organic Frameworks from Large Organic and Inorganic Secondary Building Units: New Examples and Simplifying Principles for Complex Structures. J. Am. Chem. Soc. 2001, 123 (34), 8239—8247.
- (3) Eddaoudi, M.; Moler, D. B.; Li, H.; Chen, B.; Reineke, T. M.; O'Keeffe, M.; Yaghi, O. M. Modular Chemistry: Secondary Building

- Units as a Basis for the Design of Highly Porous and Robust Metal—Organic Carboxylate Frameworks. *Acc. Chem. Res.* **2001**, 34 (4), 319—330.
- (4) Rosi, N. L.; Eckert, J.; Eddaoudi, M.; Vodak, D. T.; Kim, J.; O'Keeffe, M.; Yaghi, O. M. Hydrogen Storage in Microporous Metal-Organic Frameworks. *Science* **2003**, *300* (5622), 1127–1129.
- (5) Tranchemontagne, D. J.; Mendoza-Cortés, J. L.; O'Keeffe, M.; Yaghi, O. M. Secondary Building Units, Nets and Bonding in the Chemistry of Metal-Organic Frameworks. *Chem. Soc. Rev.* **2009**, 38 (5), 1257–1283.
- (6) Long, J. R.; Yaghi, O. M. The Pervasive Chemistry of Metal-Organic Frameworks. *Chem. Soc. Rev.* **2009**, 38 (5), 1213–1214.
- (7) Furukawa, H.; Cordova, K. E.; O'Keeffe, M.; Yaghi, O. M. The Chemistry and Applications of Metal-Organic Frameworks. *Science* **2013**, *341* (6149), 1230444.
- (8) Eddaoudi, M.; Kim, J.; Rosi, N.; Vodak, D.; Wachter, J.; O'Keeffe, M.; Yaghi, O. M. Systematic Design of Pore Size and Functionality in Isoreticular MOFs and Their Application in Methane Storage. *Science* **2002**, *295* (5554), 469–472.
- (9) Li, P.; Chen, Q.; Wang, T. C.; Vermeulen, N. A.; Mehdi, B. L.; Dohnalkova, A.; Browning, N. D.; Shen, D.; Anderson, R.; Gómez-Gualdrón, D. A.; Cetin, F. M.; Jagiello, J.; Asiri, A. M.; Stoddart, J. F.; Farha, O. K. Hierarchically Engineered Mesoporous Metal-Organic Frameworks toward Cell-Free Immobilized Enzyme Systems. *Chem.* 2018, 4 (5), 1022–1034.
- (10) Pan, Y.; Li, H.; Farmakes, J.; Xiao, F.; Chen, B.; Ma, S.; Yang, Z. How Do Enzymes Orient When Trapped on Metal—Organic Framework (MOF) Surfaces? *J. Am. Chem. Soc.* **2018**, *140* (47), 16032–16036.
- (11) Phipps, J.; Chen, H.; Donovan, C.; Dominguez, D.; Morgan, S.; Weidman, B.; Fan, C.; Beyzavi, H. Catalytic Activity, Stability, and Loading Trends of Alcohol Dehydrogenase Enzyme Encapsulated in a Metal—Organic Framework. ACS Appl. Mater. Interfaces 2020, 12 (23), 26084—26094.
- (12) Chen, Y.; Han, S.; Li, X.; Zhang, Z.; Ma, S. Why Does Enzyme Not Leach from Metal—Organic Frameworks (MOFs)? Unveiling the Interactions between an Enzyme Molecule and a MOF. *Inorg. Chem.* **2014**, *53* (19), 10006–10008.
- (13) Lian, X.; Chen, Y.-P.; Liu, T.-F.; Zhou, H.-C. Coupling Two Enzymes into a Tandem Nanoreactor Utilizing a Hierarchically Structured MOF. *Chem. Sci.* **2016**, *7* (12), 6969–6973.
- (14) Majewski, M. B.; Howarth, A. J.; Li, P.; Wasielewski, M. R.; Hupp, J. T.; Farha, O. K. Enzyme Encapsulation in Metal—Organic Frameworks for Applications in Catalysis. *CrystEngComm* **2017**, *19* (29), 4082–4091.
- (15) Lian, X.; Fang, Y.; Joseph, E.; Wang, Q.; Li, J.; Banerjee, S.; Lollar, C.; Wang, X.; Zhou, H.-C. Enzyme–MOF (Metal–Organic Framework) Composites. *Chem. Soc. Rev.* **2017**, *46* (11), 3386–3401.
- (16) Zhang, Y.; Ge, J.; Liu, Z. Enhanced Activity of Immobilized or Chemically Modified Enzymes. ACS Catal. 2015, 5 (8), 4503–4513.
- (17) Lian, X.; Erazo-Oliveras, A.; Pellois, J.-P.; Zhou, H.-C. High Efficiency and Long-Term Intracellular Activity of an Enzymatic Nanofactory Based on Metal-Organic Frameworks. *Nat. Commun.* **2017**, 8 (1), 2075.
- (18) Ruyra, À.; Yazdi, A.; Espín, J.; Carné-Sánchez, A.; Roher, N.; Lorenzo, J.; Imaz, I.; Maspoch, D. Synthesis, Culture Medium Stability, and In Vitro and In Vivo Zebrafish Embryo Toxicity of Metal—Organic Framework Nanoparticles. *Chem. Eur. J.* **2015**, *21* (6), 2508–2518.
- (19) Luzuriaga, M. A.; Welch, R. P.; Dharmarwardana, M.; Benjamin, C. E.; Li, S.; Shahrivarkevishahi, A.; Popal, S.; Tuong, L. H.; Creswell, C. T.; Gassensmith, J. J. Enhanced Stability and Controlled Delivery of MOF-Encapsulated Vaccines and Their Immunogenic Response In Vivo. ACS Appl. Mater. Interfaces 2019, 11 (10), 9740–9746.
- (20) L. Ramos, T.; Sánchez-Abarca, L. I.; Muntión, S.; Preciado, S.; Puig, N.; López-Ruano, G.; Hernández-Hernández, Á.; Redondo, A.; Ortega, R.; Rodríguez, C.; et al. MSC Surface Markers (CD44, CD73, and CD90) Can Identify Human MSC-Derived Extracellular Vesicles

- by Conventional Flow Cytometry. Cell Commun. Signal 2016, 14 (1), 2.
- (21) Brooke, G.; Cook, M.; Blair, C.; Han, R.; Heazlewood, C.; Jones, B.; Kambouris, M.; Kollar, K.; McTaggart, S.; Pelekanos, R.; Rice, A.; Rossetti, T.; Atkinson, K. Therapeutic Applications of Mesenchymal Stromal Cells. *Semin. Cell Dev. Biol.* **2007**, *18* (6), 846–858
- (22) Pittenger, M. F.; Discher, D. E.; Péault, B. M.; Phinney, D. G.; Hare, J. M.; Caplan, A. I. Mesenchymal Stem Cell Perspective: Cell Biology to Clinical Progress. *Npj Regen. Med.* **2019**, *4* (1), 1–15.
- (23) Watt, F. M.; Huck, W. T. S. Role of the Extracellular Matrix in Regulating Stem Cell Fate. *Nat. Rev. Mol. Cell Biol.* **2013**, *14* (8), 467–473.
- (24) Hynes, R. O. The Extracellular Matrix: Not Just Pretty Fibrils. *Science* **2009**, 326 (5957), 1216–1219.
- (25) Lortat-Jacob, H. The Molecular Basis and Functional Implications of Chemokine Interactions with Heparan Sulphate. *Curr. Opin. Struct. Biol.* **2009**, *19* (5), 543–548.
- (26) Brizzi, M. F.; Tarone, G.; Defilippi, P. Extracellular Matrix, Integrins, and Growth Factors as Tailors of the Stem Cell Niche. *Curr. Opin. Cell Biol.* **2012**, 24 (5), 645–651.
- (27) Klinker, M. W.; Marklein, R. A.; Lo Surdo, J. L.; Wei, C.-H.; Bauer, S. R. Morphological Features of IFN-γ-Stimulated Mesenchymal Stromal Cells Predict Overall Immunosuppressive Capacity. *Proc. Natl. Acad. Sci. U. S. A* **2017**, *114* (13), E2598–E2607.
- (28) Ijzermans, J. N.; Marquet, R. L. Interferon-Gamma: A Review. *Immunobiology* **1989**, *179* (4–5), 456–473.
- (29) Liu, Y.; Wang, L.; Kikuiri, T.; Akiyama, K.; Chen, C.; Xu, X.; Yang, R.; Chen, W.; Wang, S.; Shi, S. Mesenchymal Stem Cell–Based Tissue Regeneration Is Governed by Recipient T Lymphocytes via IFN- γ and TNF- α . Nat. Med. 2011, 17 (12), 1594–1601.
- (30) Prakash, R.; Mishra, R. K.; Ahmad, A.; Khan, M. A.; Khan, R.; Raza, S. S. Sivelestat-Loaded Nanostructured Lipid Carriers Modulate Oxidative and Inflammatory Stress in Human Dental Pulp and Mesenchymal Stem Cells Subjected to Oxygen-Glucose Deprivation. *Mater. Sci. Eng., C* **2021**, *120*, 111700.
- (31) Croitoru-Lamoury, J.; Lamoury, F. M. J.; Caristo, M.; Suzuki, K.; Walker, D.; Takikawa, O.; Taylor, R.; Brew, B. J. Interferon-γ Regulates the Proliferation and Differentiation of Mesenchymal Stem Cells via Activation of Indoleamine 2,3 Dioxygenase (IDO). *PloS One* **2011**, *6* (2), No. e14698.
- (32) Castilla-Casadiego, D. A.; Garcia, J. R.; Garcia, A. J.; Almodovar, J. Heparin/Collagen Coatings Improve Human Mesenchymal Stromal Cell Response to Interferon Gamma. *ACS Biomater. Sci. Eng.* **2019**, *5* (6), 2793–2803.
- (33) Leach, J. K.; Whitehead, J. Materials-Directed Differentiation of Mesenchymal Stem Cells for Tissue Engineering and Regeneration. *ACS Biomater. Sci. Eng.* **2018**, 4 (4), 1115–1127.
- (34) Ahmad, A.; Fauzia, E.; Kumar, M.; Mishra, R. K.; Kumar, A.; Khan, M. A.; Raza, S. S.; Khan, R. Gelatin-Coated Polycaprolactone Nanoparticle-Mediated Naringenin Delivery Rescue Human Mesenchymal Stem Cells from Oxygen Glucose Deprivation-Induced Inflammatory Stress. ACS Biomater. Sci. Eng. 2019, 5 (2), 683–695.
- (35) Zimmermann, J. A.; Hettiaratchi, M. H.; McDevitt, T. C. Enhanced Immunosuppression of T Cells by Sustained Presentation of Bioactive Interferon-γ Within Three-Dimensional Mesenchymal Stem Cell Constructs. *Stem Cells Transl. Med.* **2017**, *6* (1), 223–237.
- (36) Park, J.; Feng, D.; Zhou, H.-C. Dual Exchange in PCN-333: A Facile Strategy to Chemically Robust Mesoporous Chromium Metal—Organic Framework with Functional Groups. *J. Am. Chem. Soc.* **2015**, 137 (36), 11801–11809.
- (37) Castilla-Casadiego, D. A.; Reyes-Ramos, A. M.; Domenech, M.; Almodovar, J. Effects of Physical, Chemical, and Biological Stimulus on h-MSC Expansion and Their Functional Characteristics. *Ann. Biomed. Eng.* **2020**, *48* (2), 519–535.
- (38) Pinzon-Herrera, L.; Mendez-Vega, J.; Mulero-Russe, A.; Castilla-Casadiego, D. A.; Almodovar, J. Real-Time Monitoring of Human Schwann Cells on Heparin-Collagen Coatings Reveals

- Enhanced Adhesion and Growth Factor Response. J. Mater. Chem. B 2020, 8 (38), 8809–8819.
- (39) Cifuentes, S. J.; Priyadarshani, P.; Castilla-Casadiego, D. A.; Mortensen, L. J.; Almodóvar, J.; Domenech, M. Heparin/Collagen Surface Coatings Modulate the Growth, Secretome, and Morphology of Human Mesenchymal Stromal Cell Response to Interferon-Gamma. J. Biomed. Mater. Res., Part A 2021, 109 (6), 951–965.
- (40) Haseli, M.; Castilla-Casadiego, D. A.; Pinzon-Herrera, L.; Hillsley, A.; Miranda-Munoz, K. A.; Sivaraman, S.; Rosales, A. M.; Rao, R. R.; Almodovar, J. Immunomodulatory Functions of Human Mesenchymal Stromal Cells Are Enhanced When Cultured on HEP/COL Multilayers Supplemented with Interferon-Gamma. *Mater. Today Bio* **2022**, *13*, 100194.
- (41) Castilla-Casadiego, D. A.; Timsina, H.; Haseli, M.; Pinzon-Herrera, L.; Chiao, Y.-H.; Wickramasinghe, S. R.; Almodovar, J. Methods for the Assembly and Characterization of Polyelectrolyte Multilayers as Microenvironments to Modulate Human Mesenchymal Stromal Cell Response. ACS Biomater. Sci. Eng. 2020, 6 (12), 6626–6651.
- (42) Mbongue, J. C.; Nicholas, D. A.; Torrez, T. W.; Kim, N.-S.; Firek, A. F.; Langridge, W. H. R. The Role of Indoleamine 2, 3-Dioxygenase in Immune Suppression and Autoimmunity. *Vaccines* **2015**, 3 (3), 703–729.
- (43) Montesinos, J. J.; López-García, L.; Cortés-Morales, V. A.; Arriaga-Pizano, L.; Valle-Ríos, R.; Fajardo-Orduña, G. R.; Castro-Manrreza, M. E. Human Bone Marrow Mesenchymal Stem/Stromal Cells Exposed to an Inflammatory Environment Increase the Expression of ICAM-1 and Release Microvesicles Enriched in This Adhesive Molecule: Analysis of the Participation of TNF- α and IFN- γ . J. Immunol. Res. **2020**, 2020, 8839625.
- (44) Takikawa, O.; Kuroiwa, T.; Yamazaki, F.; Kido, R. Mechanism of Interferon-Gamma Action. Characterization of Indoleamine 2,3-Dioxygenase in Cultured Human Cells Induced by Interferon-Gamma and Evaluation of the Enzyme-Mediated Tryptophan Degradation in Its Anticellular Activity. *J. Biol. Chem.* 1988, 263 (4), 2041–2048.
- (45) Däubener, W.; Wanagat, N.; Pilz, K.; Seghrouchni, S.; Fischer, H. G.; Hadding, U. A New, Simple, Bioassay for Human IFN-Gamma. *J. Immunol. Methods* **1994**, *168* (1), 39–47.
- (46) Kwee, B. J.; Lam, J.; Akue, A.; KuKuruga, M. A.; Zhang, K.; Gu, L.; Sung, K. E. Functional Heterogeneity of IFN- γ -Licensed Mesenchymal Stromal Cell Immunosuppressive Capacity on Biomaterials. *Proc. Natl. Acad. Sci.* **2021**, *118* (35), 1–12.
- (47) Dorronsoro, A.; Lang, V.; Ferrin, I.; Fernández-Rueda, J.; Zabaleta, L.; Pérez-Ruiz, E.; Sepúlveda, P.; Trigueros, C. Intracellular Role of IL-6 in Mesenchymal Stromal Cell Immunosuppression and Proliferation. *Sci. Rep* **2020**, *10* (1), 21853.
- (48) García, J. R.; Quirós, M.; Han, W. M.; O'Leary, M. N.; Cox, G. N.; Nusrat, A.; García, A. J. IFN-γ-Tethered Hydrogels Enhance Mesenchymal Stem Cell-Based Immunomodulation and Promote Tissue Repair. *Biomaterials* **2019**, *220*, 119403.